JOURNAL OF CATALYSIS **148**, 304–314 (1994)

Hydroisomerisation–Hydrocracking of Decane over Al- and Ga-Pillared Clays

R. Molina*, S. Moreno,* A. Vieira-Coelho,* J. A. Martens,† P. A. Jacobs,† and G. Poncelet*

*Unité de Catalyse et Chimie des Matériaux Divisés, Université Catholique de Louvain, Place Croix du Sud 2/17, B-1348 Louvain-la-Neuve, Belgium; and †Centrum voor Oppervlaktechemie en Katalyse, KU Leuven, Kardinaal Mercierlaan 92, B-3001 Heverlee, Belgium

Received May 28, 1993; revised February 1994

Synthetic beidellite, natural montmorillonite, and transition metal containing clays were pillared with aluminum and transformed into bifunctional catalysts. The pillared clays with various degrees of tetrahedral substitution have been evaluated as catalysts for isomerisation–hydrocracking of decane. A comparison has been made between the catalytic properties of pillared clays and ultrastable Y zeolites. For decane isomerisation, Al-pillared beidellites and ultrastable Y zeolites are similar catalysts. The activity of the pillared clays follows the sequence of lattice tetrahedral substitution. © 1994 Academic Press, Inc.

INTRODUCTION

The first studies on the catalytic potential of Al-pillared clays were concerned with the cracking of gas–oil fractions and the upgrading of light cycle oil (1, 2). Rapid deactivation due to coke formation, insufficient acidity and poor hydrothermal stability appeared to be major drawbacks of Al-pillared clays in catalytic cracking (3, 4). In subsequent work, these handicaps were overcome with partial success by using mixed pillars such as Al–Cr (5), or hydrothermally treated pillaring solutions combining Al and Ce (6), or La (7). Additional improvements were achieved by selecting clays with higher intrinsic thermal stability, such as rectorite (8), or by contacting the clay with a solution of an alkali metal carboxylate before pillaring (9). Other approaches such as pillaring in the presence of polyvinyl alcohol (10, 11) or a surfactant (12, 13) or treating the pillared clay with a silanating agent (14), to quote a few, were also followed.

In parallel with these developments, catalytic applications were found in reactions requiring milder operating conditions or in the presence of specific pillars. Examples of such reactions are olefin oligomerisation (15), olefin synthesis from syngas (14, 16), phenol and phenol ether hydroxylation (17), unsaturated edible oil hydrogenation over Ni-pillared clays (18), MTBE synthesis (19), benzene alkylation with C_8–C_{10} olefins (20), toluene alkylation with methanol (21, 22), xylene isomerisation (23, 24), trimethylbenzene disproportionation (25–30), and biphenyl alkylation with propylene (31, 32).

The catalytic activity of Al-pillared clays seems to be largely dependent on the nature of the parent clay. In several reactions, Al-pillared beidellite was found to be more active than Al-pillared montmorillonite, e.g., in heptane hydroconversion and cumene cracking (33), in xylene isomerisation/disproportionation (24), and in biphenyl alkylation with propylene (32).

A few studies on *n*-alkane isomerisation and hydrocracking over pillared clays are available in the literature. It has been shown that Al- and Al, Cr-pillared clays constitute efficient catalysts for this type of conversion (34, 35). Parulekar and Hightower carried out the hydroconversion of pentane, hexane and heptane over Pt–Re-containing Al-pillared clays (36). Monobranched isomers were the main reaction products. Doblin *et al.* prepared platinum-containing Al-pillared clays which behaved as ideal bifunctional catalysts for octane hydroconversion (37). A high selectivity for isomerisation was obtained up to medium levels of octane conversion and the product spectrum was similar to that obtained on large pore zeolites.

The hydroconversion of *n*-alkanes over bifunctional zeolite catalysts has been extensively investigated (38–41). The balancing of the two catalytic functions and the reaction mechanisms of skeletal isomerisation and hydrocracking of alkanes in the presence and absence of molecular shape selectivity are well understood (40, 41). In the present work, a series of synthetic and natural T–O–T clays with various degrees of tetrahedral substitution were pillared with aluminum and transformed into bifunctional catalysts. They have been tested in the isomerisation and hydrocracking reactions of decane and their catalytic activities have been compared with those of ultrastable Y zeolites.

0021-9517/94 $6.00

EXPERIMENTAL

Ultrastable Y Zeolite Samples

The ultrastable Y (USY) zeolites were CBV-720 and CBV-760 from PQ. The Si/Al ratio in the framework determined with ^{27}Al MAS NMR on USY(CBV720) and USY(CBV760) amounts to 13.5 and 36, respectively. The as-received samples were in the H-form. The USY samples were impregnated with an aqueous solution of $Pt(NH_3)_4Cl_2$ to obtain a loading of 1% by weight of platinum.

Clay Samples

Four swelling clays were investigated: a homemade synthetic beidellite, the synthesis of which has been reported previously (42), a commercial natural montmorillonite, Westone L (from ECC International, U.K.), and two transition-metal-rich clays, N_4 and N_7 (from the Niquelandia deposit, Brazil).

Chemical formulas established by elemental analyses of fractions of the clays smaller than 2 μm are as follows:

Beidellite:

$$Na_{0.67}[Si_{7.33}Al_{0.67}]^{IV}[Al_4]^{VI}O_{20}(OH)_4 \cdot nH_2O$$

Montmorillonite

$$Ca_{0.22}Na_{0.02}K_{0.02}[Si_{7.94}Al_{0.06}]^{IV}$$
$$[Al_{3.20}Mg_{0.72}Fe_{0.08}]^{VI}O_{20}(OH)_4 \cdot nH_2O$$

N_4:

$$Na_{0.84}K_{0.02}Ca_{0.006}[Si_{7.60}Al_{0.40}]^{IV}$$
$$[Al_{1.04}Mg_{0.34}Fe_{2.0}Ni_{0.66}Cr_{0.12}Mn_{0.02}]^{VI}O_{20}(OH)_4 \cdot nH_2O$$

N_7:

$$Na_{0.80}K_{0.06}Ca_{0.006}[Si_{7.44}Al_{0.56}]^{IV}[Al_{0.82}Mg_{0.83}Fe_{1.37}$$
$$Ni_{0.86}Cr_{0.11}Mn_{0.005}]^{VI}O_{20}(OH)_4 \cdot nH_2O$$

Pillaring

Hydroxy–aluminum (or hydroxy–gallium) solutions were prepared by slow, dropwise addition of a 0.5 *M* NaOH solution to a 0.2 *M* solution of aluminum nitrate (or gallium nitrate). The OH/Al (or OH/Ga) molar ratio was 1.6. The solution was diluted with distilled water to obtain a 0.1 *M* Al (or Ga) concentration. The pillaring solutions were aged for 24 h at room temperature and thereafter slowly added to stirred clay suspensions (2 wt.%) using a volume of pillaring solution containing 20 meq Al (or Ga) per gram of clay.

After 24 h of equilibration, the clay suspensions were dialysed against distilled water (1 liter/g of clay), renewing the water until the electric conductivity no longer rose above its initial value of 20 μS/cm. Generally, three renewals were required. The amount of Al atoms in the pillars was close to 2 mmol/g in each sample. Further details on the pillaring can be found elsewhere (42, 43).

Finally, the clays were freeze dried. The samples will be referred to as AlPB (Al-pillared beidellite), $AlPN_4$ (Al-pillared N_4), $AlPN_7$ (Al-pillared N_7), AlPW (Al-pillared Westone L), and GaPW (Ga-pillared Westone L).

The pillared clays were impregnated with a minimum amount of an aqueous solution of $Pt(NH_3)_4Cl_2$, in order to obtain a Pt-loading of 1 wt.%, and dried at 333 K.

Characterisation of the Pillared Clays

X-ray diffraction patterns were recorded on a Philips instrument, using Ni-filtered Cu*Kα* radiation and an angle scanning speed of 2° 2θ/min. The pillared samples were calcined at 773 K before recording the X-ray diffractograms. Nitrogen adsorption isotherms were determined with a Micromeritics ASAP 2000 sorptometer on samples outgassed at 673 K for 4 h. Micropore and mesopore volumes were determined according to the methods explained in Refs. (44) and (45), respectively. The residual cation exchange capacity (CEC) of the pillared clays was derived from the nitrogen content of NH_4-exchanged samples. The nitrogen content was determined by a micro-Kjeldahl method.

The quality of the pillars is assessed by two criteria, namely (i) an interlamellar distance of 1.7 to 1.8 nm after calcination at 873–923 K, and (ii) a specific surface area of the order of 200 m^2/g. According to these two criteria, the pillaring was considered to be successful for the clays investigated (Table 1).

The Brønsted acidity of the clays was quantified using infrared spectroscopy. A self-supporting wafer of pillared clay was outgassed at 673 K for 4 h. After cooling to room temperature, dry ammonia vapor was adsorbed on the sample. Infrared spectra were recorded after evacuation at 473 K for 4 h *in vacuo*. The integrated intensity of the bending vibration band of NH_4^+ at 1440 cm^{-1}, normalised

TABLE 1

Characterisation of the Pillared Clays and Ultrastable Y Zeolites

			Pore volume			
Sample	d(001) (nm)	So (m^2/g)	Micro (cm^3/g)	Meso (cm^3/g)	Macro (cm^3/g)	Residual CEC (meq/100g)
AlPB	1.76	320	0.052	0.125	0.243	29
$AlPN_7$	1.77	177	0.057	0.090	0.021	31
$AlPN_4$	1.77	218	0.057	0.108	—	34
AlPW	1.77	206	0.074	0.122	0.085	34
GaPW	1.72	204	0.061	0.101	0.09	40
CBV-720		780	0.245	0.142	0.047	110
CBV-760		720	0.209	0.176	0.047	46

for the sample weight, was used as a measurement of the concentration of Brønsted acid sites in the sample.

Catalytic Testing

The clay and zeolite powders were compressed into flakes. Particles with diameters in the range from 0.3 to 0.5 mm were obtained by crushing these flakes and screening. An amount of 200 mg of particles was loaded into a tubular reactor with an internal diameter of 10 mm. The catalysts were activated *in situ* in the reactor by heating at 5 K/min from room temperature to 673 K under flowing oxygen. After 1 h of calcination, the catalyst bed was flushed with nitrogen and the catalyst was reduced in flowing hydrogen at the same temperature.

A stream of decane vapor in hydrogen was generated using a thermostated saturator. The molar hydrogen/decane ratio was 380, and the pressure in the reactor 0.45 MPa. The space time, W/F_0 (W being the catalyst weight and F_0, the molar flow of decane at the reactor entrance) was 1.7 kg s mmol^{-1}.

The reaction products were analysed on-line with high-resolution gas chromatography. The products were separated on a 50-m capillary CP-Sil-5 column from Chrompack and detected with FID.

RESULTS AND DISCUSSION

1. *Acidity of the Pillared Clays*

According to their chemical formulas, the starting clays exhibit two major differences, namely the degree of Al for Si substitution in the tetrahedral layers and, for the Brazilian clays, the content of transition metal elements in the octahedral layers.

It is well established that the intercalation of Al pillars in swelling clays generates Lewis and Brønsted acidity. As shown by IR spectroscopy of adsorbed pyridine, Lewis acidity associated with the Al-pillars predominates (27, 33, 46–49).

The higher activity of Al-pillared beidellite compared with Al-pillared montmorillonite was related earlier (24, 33, 42, 46) to the different nature of the Brønsted acidity in these two catalysts. Indeed, infrared spectra of H-beidellite and Al-pillared beidellite exhibit a band at 3440 cm^{-1}, attributed to Si–OH groups resulting from proton attack on tetrahedral Si–O–Al linkages (42). These Si–OH groups are relatively stable since the band at 3440 cm^{-1} is still visible after calcination at 863 K *in vacuo* (33). Upon adsorption of pyridine, the band disappears and a band at 1545 cm^{-1}, characteristic of pyridinium cations, is observed. Such observations were not noted for pillared montmorillonites. In addition, it was concluded from an IR spectroscopic study of adsorbed pyridine that the acid strength in beidellite was higher than in pillared montmorillonite (33). Therefore, the origin of the better catalytic performances of Al-pillared beidellite was assigned to tetrahedral substitutions.

A different behavior of the two types of clays was observed by Plee *et al.* (50) and Pinnavaia *et al.* (51) using ^{27}Al and ^{29}Si MAS-NMR. According to these authors, condensation reactions between the clay surface and the pillars occur in beidellite, and not in montmorillonite, and this explains the more regular distribution of pillars in beidellite (52). However, in recent work, Zheng *et al.* suggested that clay–pillar bonds are formed in both types of clays, provided that the calcination temperature exceeds 723 K (53).

In Fig. 1, the integrated intensity per gram of clay of the NH_4^+ IR band at 1440 cm^{-1}, which is proportional to the concentration of Brønsted acid sites, is plotted against the degree of isomorphic substitution in the tetrahedral layer of the parent clay materials. This figure clearly illustrates the link between proton content and degree of tetrahedral substitution.

2. *Catalytic Activity*

Isomerisation and hydrocracking of alkanes on bifunctional catalysts necessitate a cooperation of noble metal particles and Brønsted acid sites (38). The noble metal catalyses hydrogenation–dehydrogenation reactions, while isomerisation and cleavage of the hydrocarbon skeleton occurs over the Brønsted acid sites. When the two functions are well-balanced, the rearrangement of the alkenes on Brønsted acid sites is the rate-limiting step of the conversion.

Curves representing the conversion of decane obtained on the bifunctional pillared clays and USY zeolite catalysts at different reaction temperatures are shown in Fig. 2. AlPB and AlPN$_7$ exhibit similar catalytic activities and

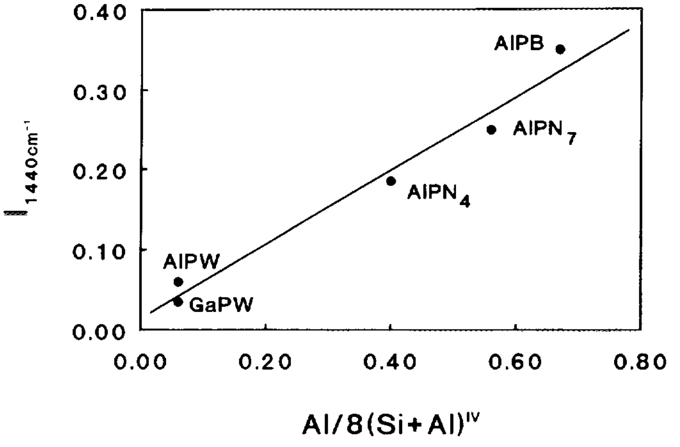

FIG. 1. Intensity of the infrared vibration band of NH_4^+ at 1440 cm^{-1} per g of Al-pillared clay versus the degree of Al substitution in the tetrahedral layers of the parent clay.

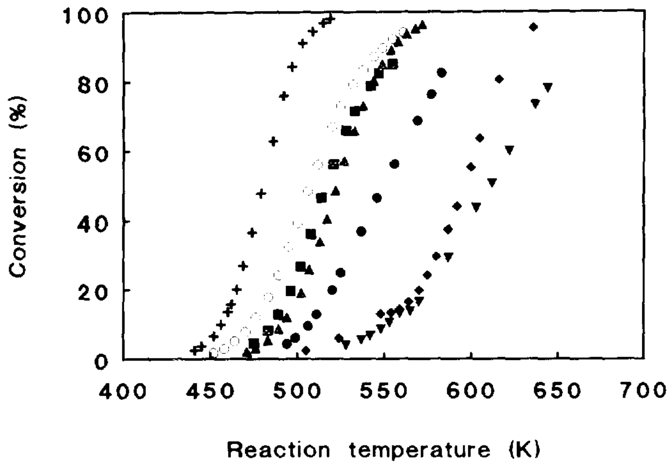

FIG. 2. Decane conversion with reaction temperature on pillared clays and USY zeolites, loaded with 1 wt.% of platinum. CBV-720 (+), AlPB (○), AlPN$_7$ (■), CBV-760 (▲), AlPN$_4$ (●), GaPW (◆), and AlPW (▼).

are substantially more active than GaPW and AlPW. On AlPB, decane is completely converted at 590 K, while on GaPW at this temperature the decane conversion reaches only 30%. GaPW is slightly more active than AlPW. The decane conversion curve for AlPN$_4$ is situated between that for AlPN$_7$ and GaPW. The catalytic activity decreases in the order

$$\text{AlPB} > \text{AlPN}_7 > \text{AlPN}_4 > \text{GaPW} > \text{AlPW}.$$

The slight differences in textural properties of the samples (Table 1) cannot explain these important differences in catalytic activity. The catalytic activity appears to be primarily determined by the Brønsted acidity (Fig. 1), as expected. The catalysts under investigation possess sufficient hydrogenation–dehydrogenation capacity for the Brønsted acidity to determine the activity. Since the number of Al pillars introduced in the different Al-pillared clay samples is comparable, the concentration of Lewis sites, associated with the pillars, is probably similar. From the relative order of catalytic activities, it may be inferred that Lewis acidity is not important in this type of catalysis, as expected.

Niquelandia clays are strictly speaking not pure beidellites, but have significant isomorphic substitution in their tetrahedral layers. Their pillared forms (AlPN$_4$ and AlPN$_7$) exhibit catalytic activities that are intermediate between those of the beidellites and montmorillonites. This result is in agreement with the work of Davidtz (54) on unpillared clays, and with the higher activity of Al-pillared saponites (a synthetic trioctahedral clay with Al for Si tetrahedral substitution) as compared to Al-pillared montmorillonites (21, 55).

The introduction of gallium instead of aluminum pillars in the montmorillonite sample does not result in a significant difference in catalytic activity, as previously observed (43).

USY(CBV-720) is substantially more active than USY(CBV-760), in agreement with its higher framework Al content. The decane conversion curves on the most active clays, AlPB and ALPN$_7$, are situated between those for the two USY zeolites (Fig. 2). The slopes of the conversion curves are steeper on the USY catalysts, indicating that the apparent activation energies are higher on the zeolites compared to the clays. On the USY samples, the apparent activation energies are 150 kJ/mol (CBV-720) and 147 kJ/mol (CBV-760); on the pillared clays 141 kJ/mol (AlPB and AlPN$_7$), 133 kJ/mol (AlPN$_4$), 90 kJ/mol (AlPW), and 79 kJ/mol (GaPW) were measured. These differences in apparent activation energies are due to a transition from bifunctional catalysis to a combination of bifunctional and monofunctional noble metal catalysis (see below).

3. *Isomerisation and Hydrocracking Yields*

In Fig. 3, the yields of decane isomerisation and hydrocracking are plotted against the degree of decane conversion. On all catalysts, isomerisation and hydrocracking are consecutive reactions. The isomerisation yield curves go through a maximum. For the clays, the maximum yield of isodecanes decreases in the order

$$\text{AlPB} > \text{AlPN}_7 > \text{AlPN}_4 > \text{AlPW} = \text{GaPW}.$$

This order corresponds to the activity order (Fig. 2) and the order of apparent activation energies. In Table 2, the isomerisation and cracking yields obtained at the isomerisation maximum are compared for the different catalysts.

High isomerisation yields are characteristic for bifunctional catalysts in which the two functions are in balance (56). The present result shows that according to this criterion the balance is realised in the AlPB and AlPN$_7$ samples.

The hydroisomerisation and hydrocracking yield curves on AlPB are similar to those obtained on the USY zeolites. The maximum yield of isodecanes on AlPB is 61.7%. On the USY zeolites, it is 59.2% (CBV-760) and 59.9% (CBV-720). The latter values correspond to the highest values reported in the literature for decane isomerisation yields obtained with Y type zeolites (57).

4. *Isomerisation Selectivity*

The distribution of isodecanes according to their degree of branching is presented in Fig. 4. On all catalysts, mono-, di-, and tri-branched isodecanes are formed in consecutive reactions. This feature is explained by a formation of side chains in the carbon skeleton through protonated cycloalkane intermediates (40). Tribranched iso-

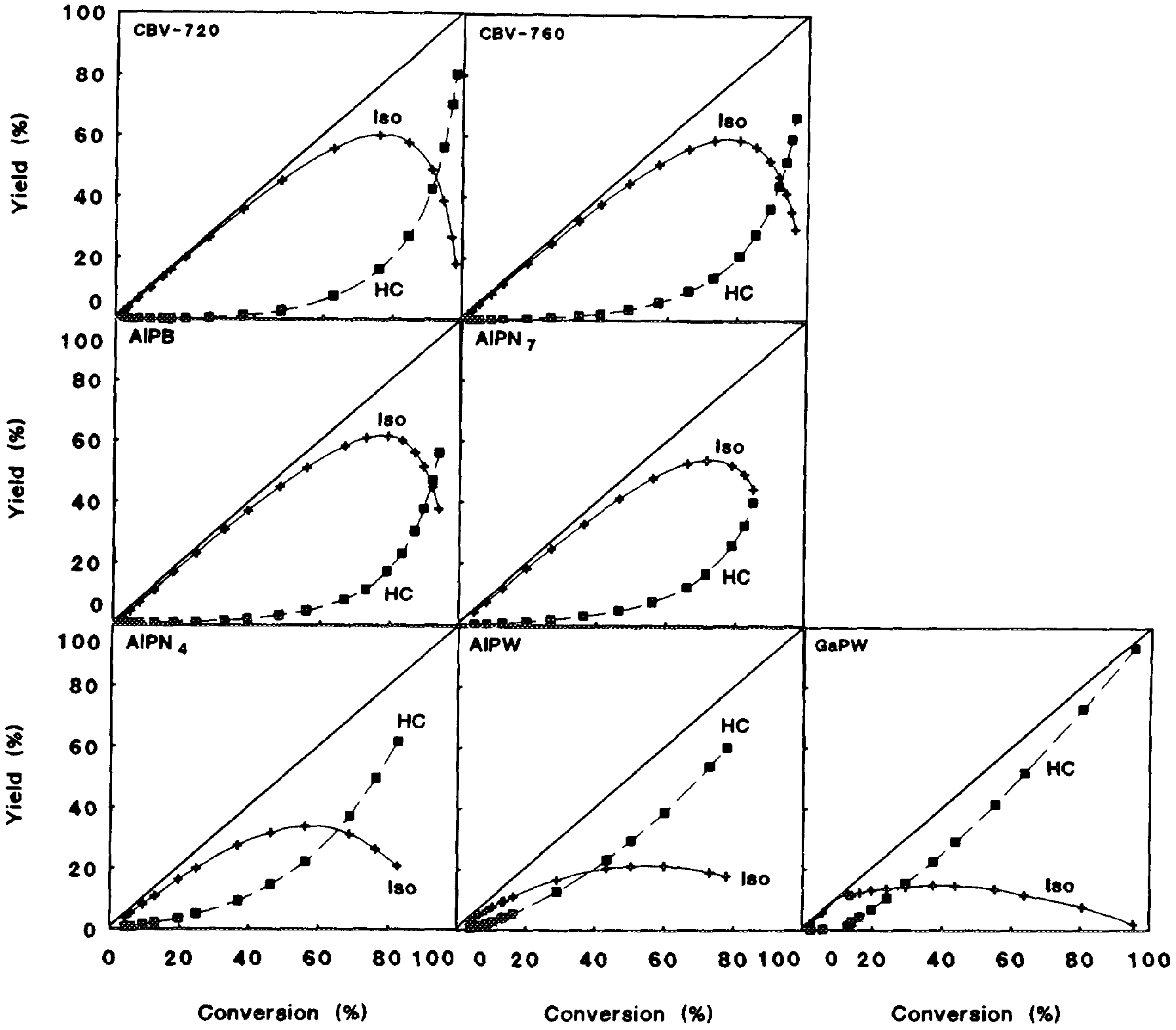

FIG. 3. Yield of isomerisation (Iso) and hydrocracking (HC) of decane.

TABLE 2

Yields of Isomers and Cracked Products at Maximum Isomerisation Yield

Catalyst	Temperature (K)	Conversion (%)	Yield of isomers (%)	Yield of cracked products (%)	Isomerisation selectivity (%)	Isomerisation selectivity at 60% conversion
AlPB	532	79.2	61.7	17.6	77.9	89.7
AlPN$_7$	533	71.5	54.2	17.2	75.8	83.6
AlPN$_4$	556	56.2	33.9	22.3	60.3	55.2
AlPW	622	60.0	21.1	38.9	35.2	35.2
GaPW	587	37.4	14.8	22.6	39.6	20.7
CBV-720	492	76.0	59.9	16.2	78.8	89.2
CBV-760	544	80.3	59.2	21.1	73.7	88.0

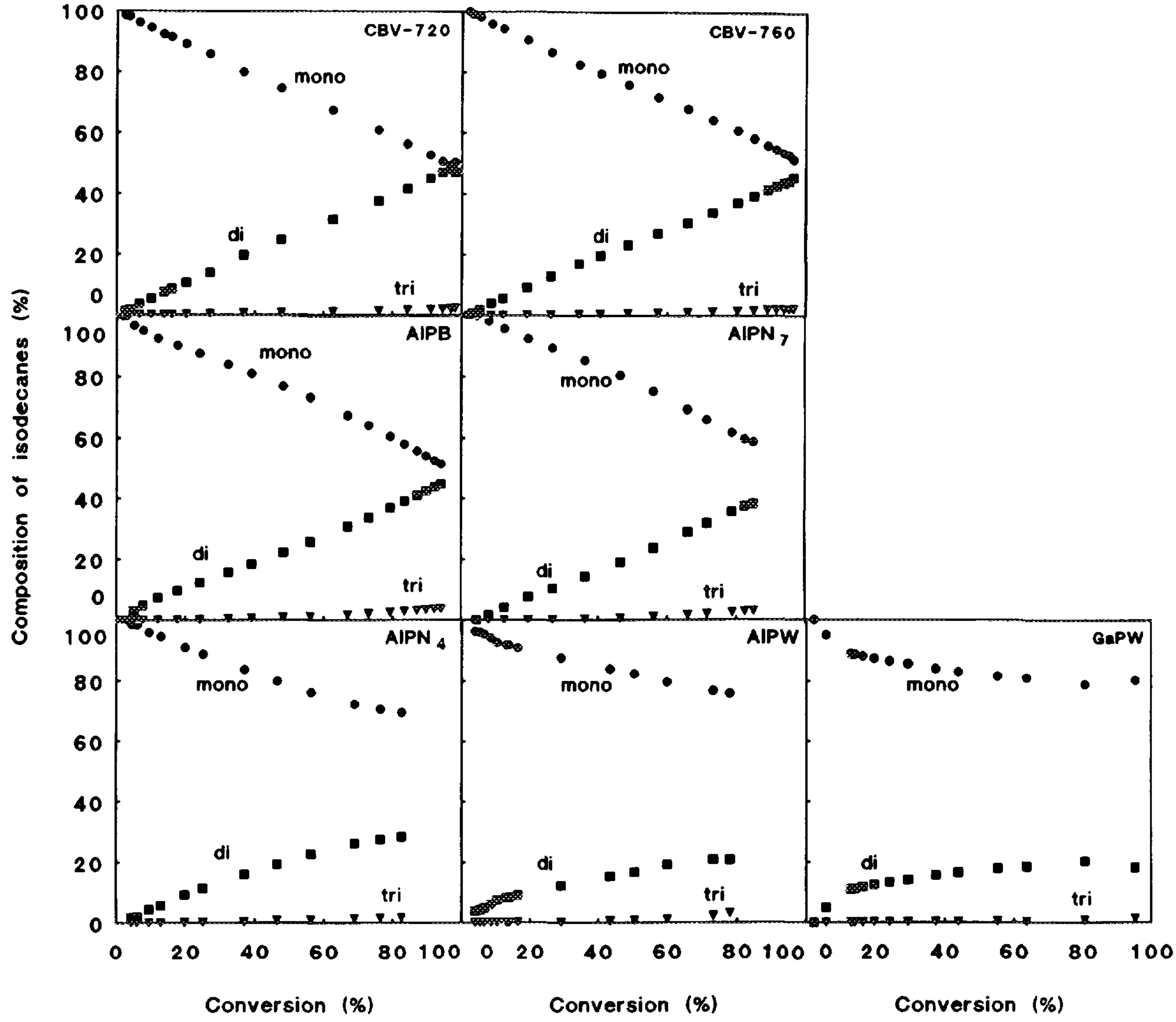

FIG. 4. Distribution of the isodecanes according to the number of branchings in their carbon skeleton versus decane conversion.

decanes are obtained in small amounts. The curves for the most active clays, AlPB, AlPN$_7$, and AlPN$_4$, are very similar to those obtained on the USY zeolites (Fig. 4). Tribranched isomers are slightly more abundant on the AlPB and AlPN$_7$ clays (Table 3).The isodecanes obtained on montmorillonites (AlPW and GaPW) contain less di- and tri-branched isomers (Table 3).

The distribution of the monobranched isodecanes according to the nature of the side chain is shown in Fig. 5. All possible monobranched isodecanes are formed, namely 2-, 3-, 4-, and 5-methylnonane, 3- and 4- ethyloctane, and 4-propylheptane. The methylnonanes are formed mainly through cyclisation and ring reopening in protonated alkylcyclopropane intermediates. On USY catalysts, at least part of the ethyloctanes and 4-propylheptane are primary products (54). Reaction schemes for their direct formation from *n*-decane involve protonated

TABLE 3

Distribution of the Mono-, Di-, and Tribranched Isomers Obtained at Maximum Isomerisation Yield

Catalyst	Yields of isomers at max. isom. (%)	Distribution (%)		
		mono-	di-	tri-
AlPB	61.7	60.6	36.9	2.5
AlPN$_7$	54.2	66.2	31.9	2.0
AlPN$_4$	33.9	76.3	22.8	1.0
AlPW	21.1	79.8	19.2	1.1
GaPW	14.8	84.1	15.7	0.3
CBV-720	59.9	60.9	37.7	1.4
CBV-760	59.2	61.1	37.4	1.6

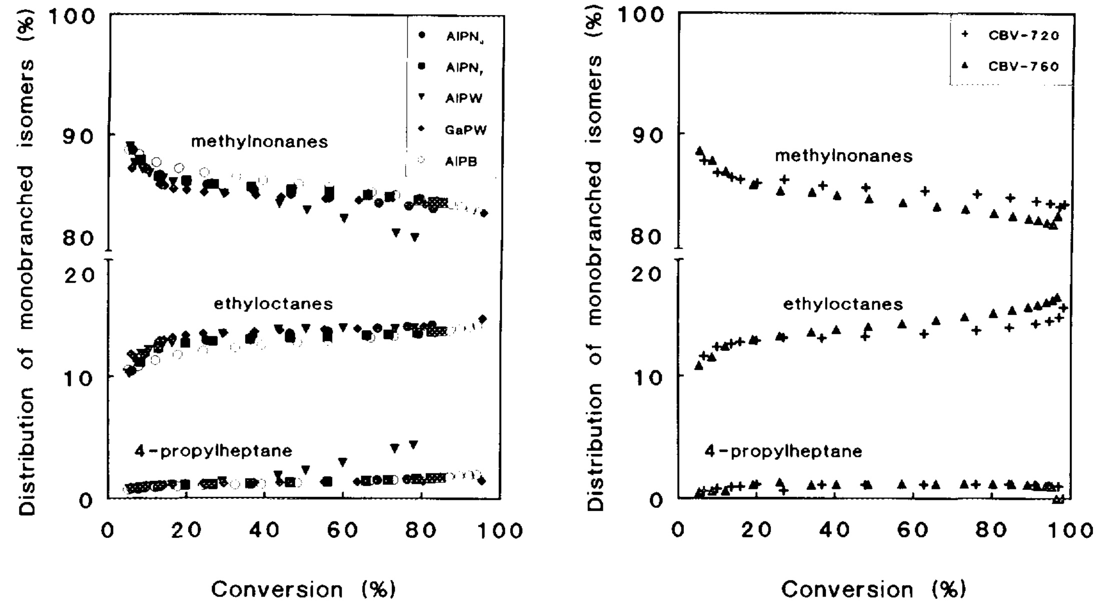

FIG. 5. Distribution of monobranched isodecanes according to the size of the side chain versus decane conversion.

alkylcycloalkanes with cyclobutane and cyclopentane rings (58). The decane monobranching patterns on pillared clays and USY zeolites are strikingly similar (Fig. 5).

The distribution of the individual methylnonane isomers is shown in Fig. 6 for AlPB and CBV-720. A suppressed formation of 2-methylnonane and an enhanced formation 5-methylnonane at low conversion are features of methylbranching via protonated alkylcyclopropane intermediates (59). This behavior is observed on the USY catalysts. The distribution of methylnonanes obtained on AlPB (Fig. 6) is representative for all clay samples investigated. On the clay catalysts, the distribution of the methylnonanes does not change with conversion and corresponds to the thermodynamic equilibrium for these isomers. Assuming the same mechanism for branching isomerisation on both types of catalysts, the results of Fig. 6 suggest that methyl shifts are faster on clays compared to USY catalysts.

In the chromatographic analysis of the reaction products, 4-ethyloctane and 2,3-dimethyloctane are not always sufficiently resolved. They are thus considered together in Fig. 7, in which the composition of the ethyloctane product fraction is plotted against decane conversion. The molar 3-ethyloctane/(4-ethyloctane + 2,3-dimethyloc-

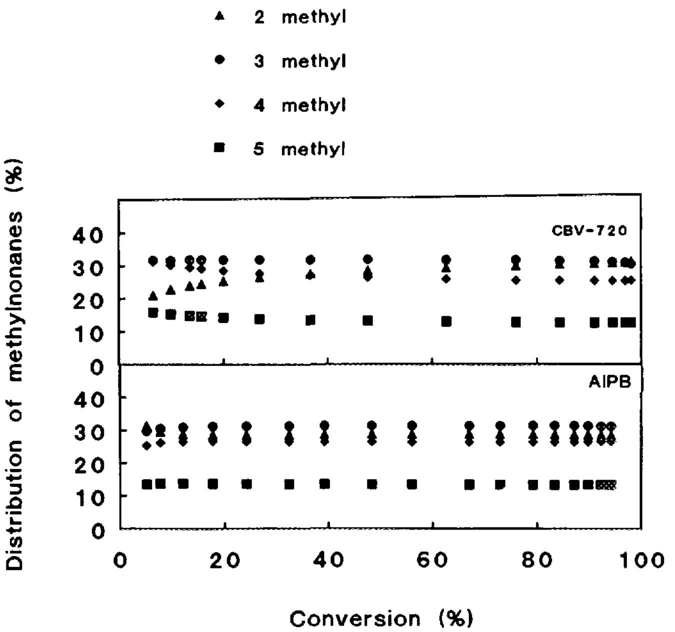

FIG. 6. Distribution of the individual methylnonanes versus decane conversion on AlPB and CBV-720.

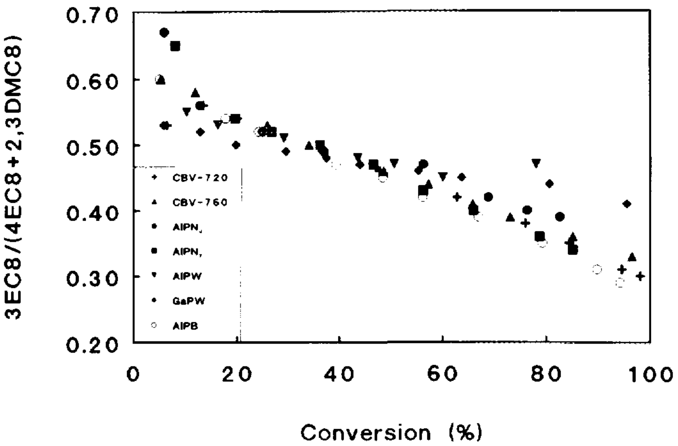

FIG. 7. Product ratio of 3-ethyloctane/(4-ethyloctane + 2,3-dimethyloctane) versus decane conversion.

TABLE 4

Distribution of Dibranched Isodecanes at Medium Conversion of Decane[a]

Catalyst	Conversion of *n*-C10 (%)	Yield of DB-C10 (%)	2,2 DMC8	2,4 DMC8	2,5 DMC8	3,5 DMC8	2,6 DMC8	2,7 DMC8	3,6 DMC8	3,3 DMC8	3,4 DMC8	4,4 DMC8	4,5 DMC8	3E,4M C7
AlPB	48.3	9.1	3.4	15.2	21.9	5.1	22.4	15.1		13.1		1.8	1.5	0.4
AlPN$_7$	46.5	7.2	3.4	15.5	22.1	5.6	21.6	14.4		13.4		1.9	1.7	0.5
AlPN$_4$	46.4	5.6	3.4	15.0	21.9	5.6	21.2	14.4		0.7	13.6	1.9	1.8	0.5
AlPW	50.5	3.0	3.5	13.6	20.4	5.6	19.6	15.6		1.3	13.8	1.6	4.4	0.6
GaPW	55.2	2.1	3.5	14.4	22.4	6.0	20.6	14.6		15.1		1.3	2.1	0.0
CBV-720	47.7	10.4	3.4	19.4	19.0	5.6	18.3	6.9	3.2	6.7	9.7	3.7	2.4	1.8
CBV-760	48.5	9.7	3.6	18.7	18.8	5.7	18.3	6.6	3.2	6.6	9.8	3.6	2.8	2.2

[a] 2,3DMC8 was not always resolved from 4EC8 and is not contained in the distribution; DB-C10 stands for dibranched isodecanes, DMC8 for dimethyloctane, 3E,4MC7 for 3-ethyl-4-methylheptane, and 4EC8 for 4-ethyloctane.

tane) product ratio is similar on all types of catalysts investigated (Fig. 7).

Distributions of dibranched isodecanes obtained at medium levels of conversion are compared in Table 4. Dibranched isomers with the two side chains separated by two or more methylene groups (2,5-DMC8, 2,6-DMC8, 2,7-DMC8, and 3,6-DMC8) in the main chain are slightly more abundant on clays than on USY zeolites. On USY

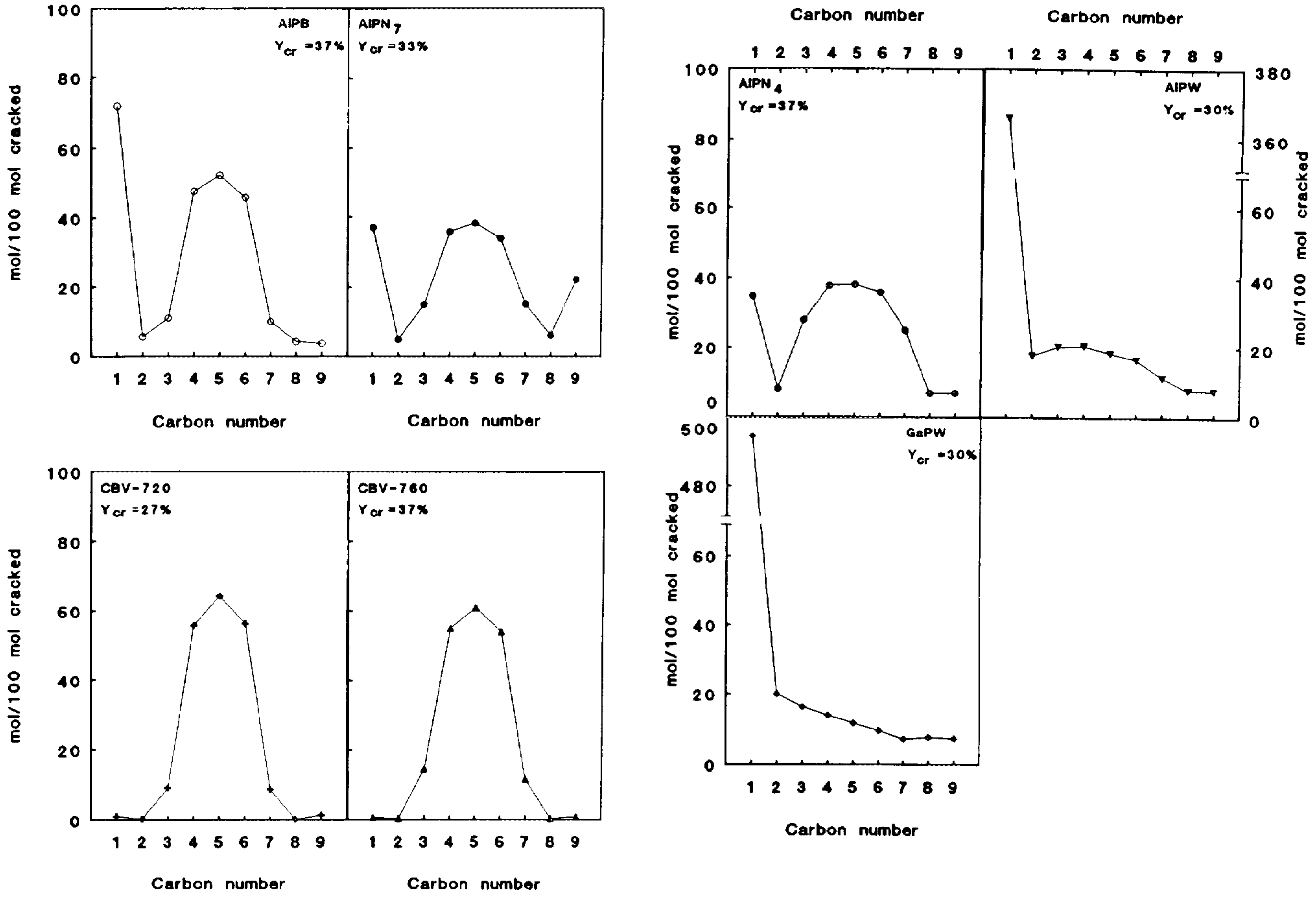

FIG. 8. Hydrocracking selectivity for the different carbon number fractions of the cracked products (mol/100 mol of feed cracked) at medium hydrocracking conversion.

catalysts, the dibranched isodecanes are distributed according to the thermodynamic equilibrium (40). The deviations from this distribution observed on clay catalysts are interpreted as an effect of molecular shape selectivity in the interlamellar microvoids. Since the kinetic diameters of the dibranched isomers are similar, the molecular shape selectivity effect should be of the transition-state type rather than of the diffusional type.

4. *Hydrocracking Selectivity*

As discussed by Weitkamp (56), only primary fragmentation is expected to occur under ideal hydrocracking conditions, when the balance between metal and acid functions is respected. In terms of carbon numbers of products, primary hydrocracking of decane is associated with identical selectivities for C_3 and C_7 fragments, as well as for C_4 and C_6 fragments.

Hydrocracking selectivities (expressed in moles per 100 moles of decane cracked) at medium hydrocracking conversions are shown in Fig. 8. The clays produce methane, which is indicative of the occurrence of hydrogenolysis on platinum. Based on the extent of methane formation, hydrogenolysis is the main cracking mechanism on AlPW and GaPW. Deviation from primary hydrocracking can be monitored by differences in the number of moles of C_3 and C_7 (Fig. 9) and of C_4 and C_6 (Fig. 10) produced. Primary cracking is considered to occur when these differences do not exceed approximately 2 mol/100 mol cracked. The AlPB, $AlPN_7$, and $AlPN_4$ clay materials show symmetric cracked product distributions up to 40% cracking conversion. On AlPW and GaPW, the cracked product distributions are always asymmetric. On USY(720), primary cracking occurs at all levels of hydrocracking, in agreement with literature data (60). USY(CBV-760) shows some contribution of secondary cracking at low levels of hydrocracking.

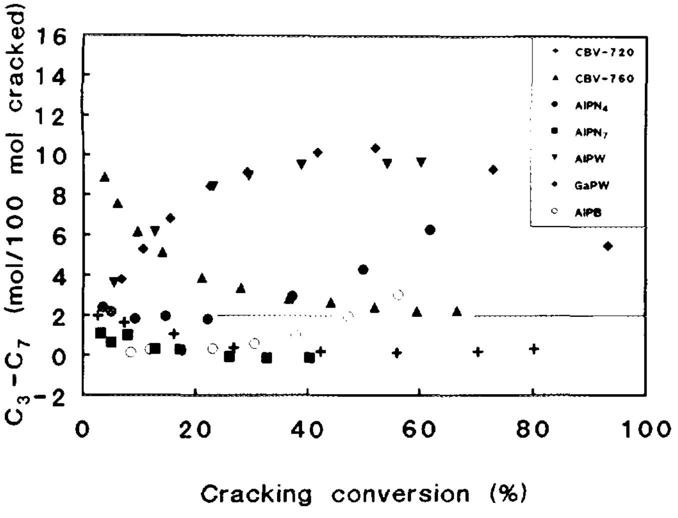

FIG. 9. Difference in cracked product selectivity for C_3 and C_7 fractions (mol/100 mol cracked) against hydrocracking conversion.

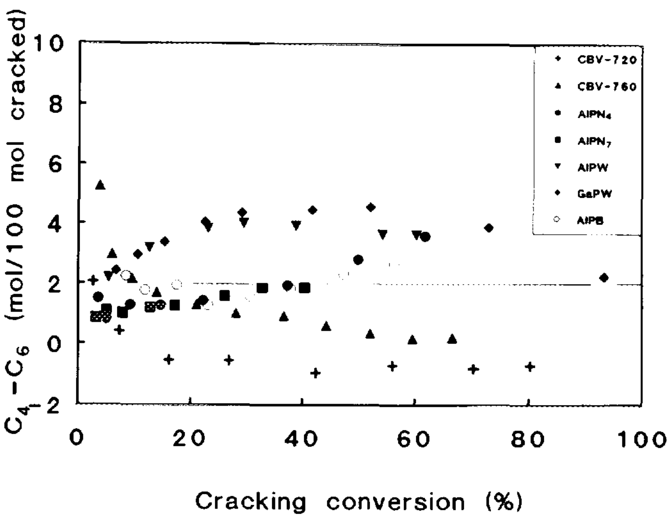

FIG. 10. Difference in cracked product selectivity for C_4 and C_6 fractions (mol/100 mol cracked) against hydrocracking conversion.

The content of branched products in the different carbon number fractions of the cracked products at medium levels of hydrocracking is plotted in Fig. 11. On the USY zeolites, the cracked products are mostly branched. The degree of branching is highest in the C_7 fraction. The same observation was made previously for bifunctional CaY (61) and USY (39) zeolites, and rationalised in terms of the β-scission mechanism (39). On the clay catalysts, the isomer content of the carbon number fractions decreases in the catalyst order

$$\mathrm{AlPB} > \mathrm{AlPN}_7 > \mathrm{AlPW} = \mathrm{AlPN}_4 = \mathrm{GaPW}.$$

This order reflects the acidity of the clays (Fig. 1) and points to an increasing contribution of hydrogenolysis. It

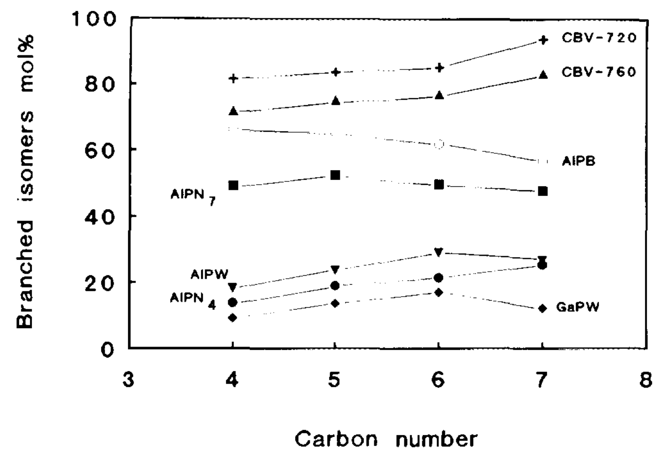

FIG. 11. Isomer content (%) in C_4 to C_7 cracked product fractions, obtained at ca. 50% hydrocracking conversion.

remains to be investigated whether the noble metal function can be tuned in the clays in order to suppress hydrogenolysis.

CONCLUSIONS

In isomerisation and hydrocracking of decane, the catalytic properties of Al-pillared clays are markedly influenced by the nature of the starting clay. There exists a direct relationship between the catalytic activity and the Brønsted acidity, associated with Al for Si substitution in the tetrahedral layers. The Brønsted acidity which is generated in montmorillonites by introducing Al-pillars is insufficient for achieving bifunctional properties.

The catalytic activity of Al-pillared beidellite is situated between that of USY samples with framework Si/Al ratios of 13.5 and 30. The product distributions from decane isomerisation over Al-pillared beidellite are very similar to those obtained with USY. It is concluded that USY and Al-pillared beidellite are similar isomerisation catalysts. The isomerisation properties are lost when the degree of Al for Si substitution in the tetrahedral layer of the clay is diminished. On USY zeolites containing 1 wt.% of platinum metal, hydrogenolysis is absent, primary hydrocracking is obtained and the cracked products are essentially branched. On the pillared clays containing the same amount of noble metal, hydrogenolysis is superimposed on hydrocracking and the contribution of it increases with decreasing Brønsted acidity. Apparently, the tuning of the two functions is pillared clays is more critical and difficult to achieve than in USY zeolites.

ACKNOWLEDGMENTS

Two of us (S. M. and R. M.) appreciate receiving financial support from the CGRI (Commissariat Général aux Relations Internationales, Belgique) and Colciecias (Colombia), respectively. J. A. M. acknowledges the Flemish National Science Foundation (NFWO) for a research position as Senior Research Associate.

REFERENCES

1. Lussier, R. J., Magee, J. S., and Vaughan, D. E. W., Preprints 7th Canadian Symposium on Catalysis, 88 (1980).
2. Occelli, M. L., *Ind. Eng. Chem. Prod. Res. Dev.* **22,** 553 (1983).
3. Occelli, M. L., and Lester, J. E., *Ind. Eng. Chem. Prod. Res. Dev.* **24,** 27 (1985).
4. Occelli, M. L., Innes, R. A., Hwu, F. S. S., and Hightower, J. W., *Appl. Catal.* **14,** 69 (1985).
5. Carrado, K. A., Suib, S. L., Skovlarikis, N. D., and Coughlin, R. W., *Inorg. Chem.* **25,** 4217 (1986).
6. McCauley, J. R., Int. Pat. Appl. PCT/US88-00567, (1988).
7. Sterte, J., *Clays Clay Miner.* **39,** 167 (1991).
8. Jingjie, G., Enze, M., and Zhiging, Y., Eur. Pat. 197.012 (1986).
9. Harris, J. R., Battiste, D. R., and Bertus, B. J., US Pat. 4,742,033 (1988).
10. Suzuki, K., Mori, T., Kawase, K., Sakami, H., and Iida, S., *Clays Clay Miner.* **36,** 147 (1988).
11. Suzuki, K., and Mori, T., *Appl. Catal.* **63,** 181 (1990).
12. Fahey, D. R., Williams, K. A., Harris, J. R., and Stapp P. R., US Pat. 4,845,066 (1989).
13. Michot, L., and Pinnavaia, T. J., *Chem. Mater.* **4,** 1433 (1992).
14. Landau, S. D., and Hinnenkamp, J. A., US Pat. 4,963,518 (1990).
15. Kukes, S. G., Banks, R. L., and Harris, J. R., US Pat. 4,879,425 (1989).
16. Mari, D., Barrault, J., Zivkov, C., Van Damme, H., and Hassoun, N., Fr. Pat. 2,617,739 (1989).
17. Constantini, M., Eur. Pat. 299,893 (1988).
18. Landau, S. D., and Hinnenkamp, J. A., US Pat. 5,037,787 (1991).
19. Atkins, M. P., Eur. Pat. 249,352 (1987).
20. Kocal, J. A., US Pat. 5,034,564 (1991).
21. Urabe, K., Sakurai, H., and Izumi, Y., *J. Chem. Soc., Chem. Commun.*, 1074 (1986).
22. Horio, M., Suzuki, K., Masuda, H., and Mori T., *Appl. Catal.* **72,** 109 (1991).
23. Mori, T., and Suzuki, K., *Chem. Lett.* 2165 (1989).
24. Molina, R., Schutz, A., and Poncelet, G., *J. Catal.* **145,** 79 (1994).
25. Kikuchi, E., Matsuda, T., Ueda, J., and Marita, Y., *Appl. Catal.* **16,** 401 (1985).
26. Kikuchi, E., Matsuda, T., Fujiki, H., and Morita, Y., *Appl. Catal.***11,** 331 (1984).
27. Matsuda, T., Asanuma, M., and Kikuchi, E., *Appl. Catal.* **38,** 289 (1985).
28. Matsuda, T., Fuse, T., and Kikuchi, E., *J. Catal.* **106,** 38 (1987).
29. Kojima, M., Hartford, R., and O'Connor, T., *J. Catal.* **128,** 487 (1991).
30. Ko, A. N., and Hsin-Chuan Chang, *J. Chin. Chem. Soc.* **30,** 81 (1992).
31. Butruille, J. R., and Pinnavaia, T. J., *Catal. Lett.* **12,** 187 (1992).
32. Remy, M., and Poncelet, G., in preparation.
33. Poncelet, G., and Schutz, A., *in* "Chemical Reactions in Organic and Inorganic Constrained Systems" (R. Setton, Ed.), p. 165. Reidel, Dardrecht, 1986.
34. Jacobs, P., Poncelet, G., and Schutz, A., Eur. Pat. 79718 (1982).
35. Plee, D., Schutz, A., Borg, F., Jacobs, P., Poncelet, G., Gatineau, L., and Fripiat, J. J., Fr. Pat. 2,563,446 (1984).
36. Parulekar, V. N., and Hightower, J. W., *Appl. Catal.* **35,** 249 (1987).
37. Doblin, C., Mathews, J. F., and Turney, T. W., *Appl. Catal.* **70,** 197 (1991).
38. Weitkamp, J., *in* "Hydrocracking and Hydrotreating" (J. W. Ward and S. A. Qader, Eds.), ACS Symposium Series Vol. 20, p. 1, 1975.
39. Martens, J. A., Jacobs, P. A., and Weitkamp, J., *Appl. Catal.* **20,** 239 (1986).
40. Martens, J. A., and Jacobs, P. A., *in* "Theoretical Aspects of Heterogeneous Catalysis" (J. B. Moffat, Ed.), p. 52. Van Nostrand–Reinhold, New York, 1990.
41. Martens, J. A., Tielen, M., Jacobs, P. A., and Weitkamp, J., *Zeolites* **4,** 98 (1984).
42. Schutz, A., Stone, W. E. E., Poncelet, G., and Fripiat, J. J., *Clays Clay Miner.* **35,** 251 (1987).
43. Vieira-Coelho, A., and Poncelet, G., *in* "Pillared Layered Structures: Current Trends and Applications" (I. V. Mitchell, Ed.), p. 185. Elsevier, New York, 1990.
44. de Boer, J.H., Lippens, B. C., Linsen, B. G., and Osinga, T. V., *J. Colloid Interface Sci.* **21,** 405 (1966).
45. Barrett, E. P., Joyner, L. G., and Halenda, P. P., *J. Am. Chem. Soc.* **73,** 373 (1951).
46. Schutz, A., Plee, D., Borg, F., Jacobs, P., Poncelet, G., and Fripiat, J. J., *in* "Proceedings, International Clay Conference" (L. G. Schutz, H. van Olphen, and F. A. Mumpton, Eds.), p. 305. The Clay Miner. Soc., 1987.

47. Occelli, M. L., and Tindwa, R. M., *Clays Clay Miner.* **31,** 22 (1983).
48. Shabtai, J., Massoth, F. E., Tokarz, M., Tsai, G. M., and McCauley, J., *in* "Proceedings, 8th International Congress on Catalysis, Berlin, 1984," p. 735. Dechema, Frankfurt-am-Main, 1984.
49. Tichit, D., Fajula, F., Figueras, F., Bousquet, J., and Gueguen, C., *in* "Catalysis by Acids and Bases" (B. Imelik *et al.*, Eds), Elsevier, Amsterdam, p. 391. 1985.
50. Plee, D., Borg, F., Gatineau, L., and Fripiat, J. J., *J. Am. Chem. Soc.* **107,** 2362 (1985).
51. Pinnavaia, T. J., Landau, S. D., Tzou, M. S., and Johnson, I. D., *J. Am. Chem. Soc.* **107,** 7222 (1985).
52. Plee, D., Gatineau, L., and Fripiat, J. J., *Clays Clay Miner.* **35,** 81 (1987).
53. Zheng, L., Mao, Y., Tao, L., Zheng, Y., and Xua, Z., *Zeolites* **12,** 374 (1992).
54. Davidtz, J. C., *J. Catal.* **43,** 260 (1976).
55. Molina, R., and Poncelet, G., to be published.
56. Weitkamp, J., *Erdoel Kohle, Erdgas, Petrochem. Brennst.-Chem.* **31,** 13 (1978).
57. Martens, J. A., and Jacobs, P. A., *J. Mol. Catal.* **78,** L47 (1993).
58. Martens, J. A., and Jacobs, P. A., *J. Catal.* **124,** 357 (1990).
59. Weitkamp, J., *Ind. Eng. Chem. Prod. Res. Dev.* **21,** 550 (1982).
60. Steijns, M., Froment, G., Jacobs, P., Uytterhoeven, J., and Weitkamp, J., *Ind. Eng. Chem. Prod. Res. Dev.* **20,** 654 (1981).
61. Weitkamp, J., Jacobs, P. A., and Martens, J. A., *Appl. Catal.* **8,** 123 (1983).